# Performance Analysis and Enhancement of Free Space Optical Links for Developing State-of-the-Art Smart City Framework

**Sonali Chauhan [1], Rajan Miglani [1], Lavish Kansal [1], Gurjot Singh Gaba [1] and Mehedi Masud [2,\*]**

[1] Department of Electronics & Electrical Engineering, Lovely Professional University, Phagwara 144411, India; chauhansonali4@gmail.com (S.C.); rajan.16957@lpu.co.in (R.M.); lavish.kansal@lpu.co.in (L.K.); gurjot.17023@lpu.co.in (G.S.G.)

[2] Department of Computer Science, College of Computers and Information Technology, Taif University, P.O. Box 11099, Taif 21944, Saudi Arabia

\* Correspondence: mmasud@tu.edu.sa

**Abstract:** In this paper, we have investigated and reported the performance of free-space optical (FSO) links operating in adverse atmospheric conditions. Since FSO links share operational similarity with fiber communication; hence, we believe that a cost-effective FSO framework can play a significant role in the transparent integration of high-speed network access backbones with the end-users. Different modulation formats, complemented with spatial diversity techniques, are discussed in this paper to strategize performance optimization of FSO links. Using bit error rate (BER) and signal-to-noise ratio (SNR) as performance metrics, it was found that binary phase-shift keying (BPSK) qualifies as the best technique modulation technique delivering SNR gain of 10 dB over on–off keying (OOK) operating link under similar channel conditions. Further performance optimization was achieved using space diversity reception wherein SNR witnessed a gain of 3 dB gain over the single-channel FSO link. In terms of application, the proposed model can help in developing a citizen-centric smart city ecosystem that can support seamless communication between heterogeneous smart devices.

## 1. Introduction

### 1.1. Preliminaries

Over the past few years, communication technology and related innovations have taken a huge leap in transforming the meaning of connectivity. Today we are surrounded by a range of diverse communication technologies like smartwatches, smartphones and smart T.V., etc., to name a few, and all such devices demand seamless data connectivity for an optimized and rich user experience. With the exponential growth of data demand and an anticipated similar aggressive trend in the near future, it is believed that existing radio-frequency (RF) infrastructure will face an acute spectrum shortage in coping with the exponential increase in user data demands [1–4]. The advent of optical fiber communication or light-wave communication as it may be commonly known is, although a promising contender in delivering high-speed data networks, then it falls short on key features like end-user mobility. Furthermore, installation and maintenance costs of optical fiber links make them economically unviable for the majority of the end-users, and it is for the same reason that despite being within a mile distance from fiber networks, approximately 75% of households in North America do

not have access to fiber bandwidth [4–6]. As shown in Figure 1, free-space optical communication, which essentially a subclass of optical wireless communication (OWC) technology, uses the atmosphere as an unguided medium for the propagation of optically modulated information signal. Using a set of electrical-to-optical and optical-to-electrical circuits, FSO systems are capable of transmitting user information onto an optical carrier and then convert back to the electrical domain at the receiver. Since the underlying hardware and transmission mechanism used in FSO systems is very much the same as in light-wave networks, hence the FSO links are capable of delivering high-speed access of the order of Gbps to the end-users [1,4,6]. Miscellaneous advantages of FSO link include: (a) plug-and-play installation behavior, (b) installations costs approximately 1/10th of the fiber links, (c) ultra-wide bandwidth, (d)unmatched user data security, and (e) license-free spectrum [1,7,8].
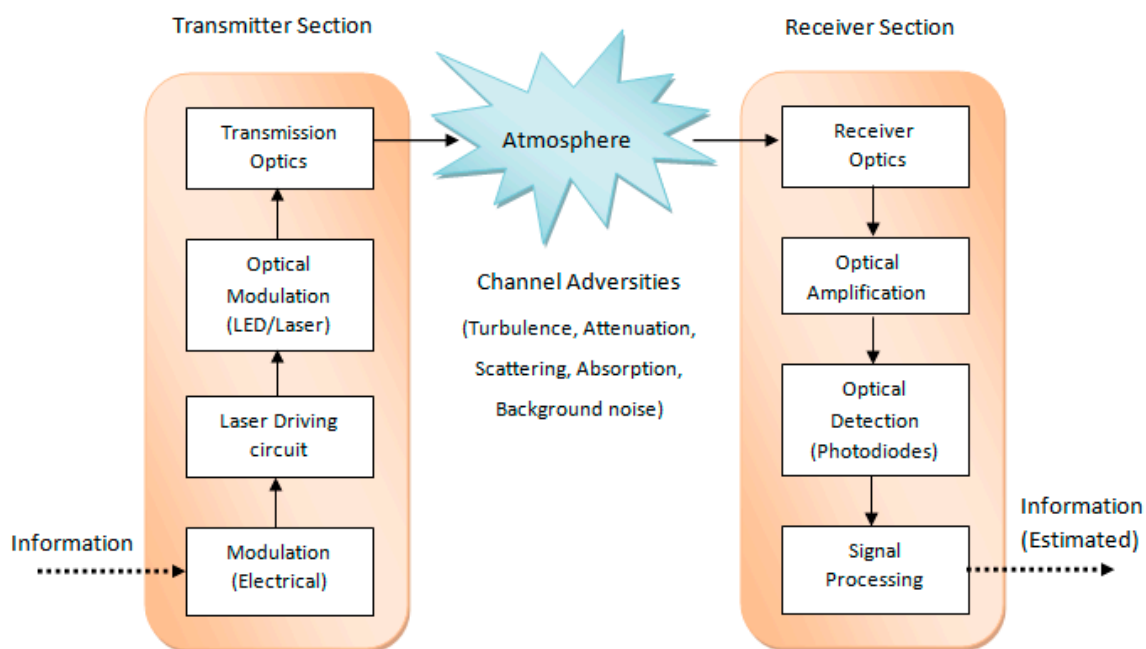


**Figure 1.** Block diagram of signal modulation, propagation and detection in free-space optics (FSO) link.

Rising urbanization, population expansion, elevated living costs and desire for better living standards has created an urgent need for optimum usage of resources through the creation of smart cities. Smart cities are designed to look after the welfare of their citizens through the optimum distribution of benefits while ensuring sustained development. An intelligent traffic system is one such example wherein the traffic lights are managed dynamically to ensure a smooth and safe flow of traffic, thus reducing commuting time and carbon emissions. Figure 2 illustrates a smart city framework in which FSO links have been proposed to serve citizens with high-speed data access in different possible ways. Case A, for example, shown in Figure 2, illustrates end-to-end optical bandwidth connectivity to far-flung and remote locations through the use of FSO relay nodes. Since FSO links can be used as plug and play devices with line-of-sight (LOS) connectivity hence, in adverse geographical conditions where installing RF links or digging earth for laying fibers is an arduous task, FSO links can serve as an ideal solution. The use of amplify-and-forward relay nodes to connect end-users with fiber backbone has also been proposed in [7]. Another possible application of FSO systems towards smart cities can be developing intelligent traffic mechanisms. The hybrid-FSO links have been previously shown to be interoperable with RF and visible light communication (VLC) standards [9]. Case B, shown in Figure 2, proposes the application of FSO to serve fast-moving traffic and pedestrians with data connectivity through RF and VLC links. The data aggregation of traffic intensity through technology feature such as the Internet of things (IoT) can be used to manage service lanes, traffic lights and related infrastructure to ensure smooth traffic flow [9–11]. The third and most significant application will be

that of cost-effective data connectivity to residential/individual users. Here as well, in case C, the FSO operating in the 780–1600 nm range can be downconverted to the VLC spectrum range, i.e., 375–700 nm, thus providing end-users optical connectivity. Thus, in the different examples shown in Figure 2, FSO links can be used to extend the optical carrier used in the existing high-capacity fiber backbone and core network to the end-users with having the need to install an expensive light-wave network.
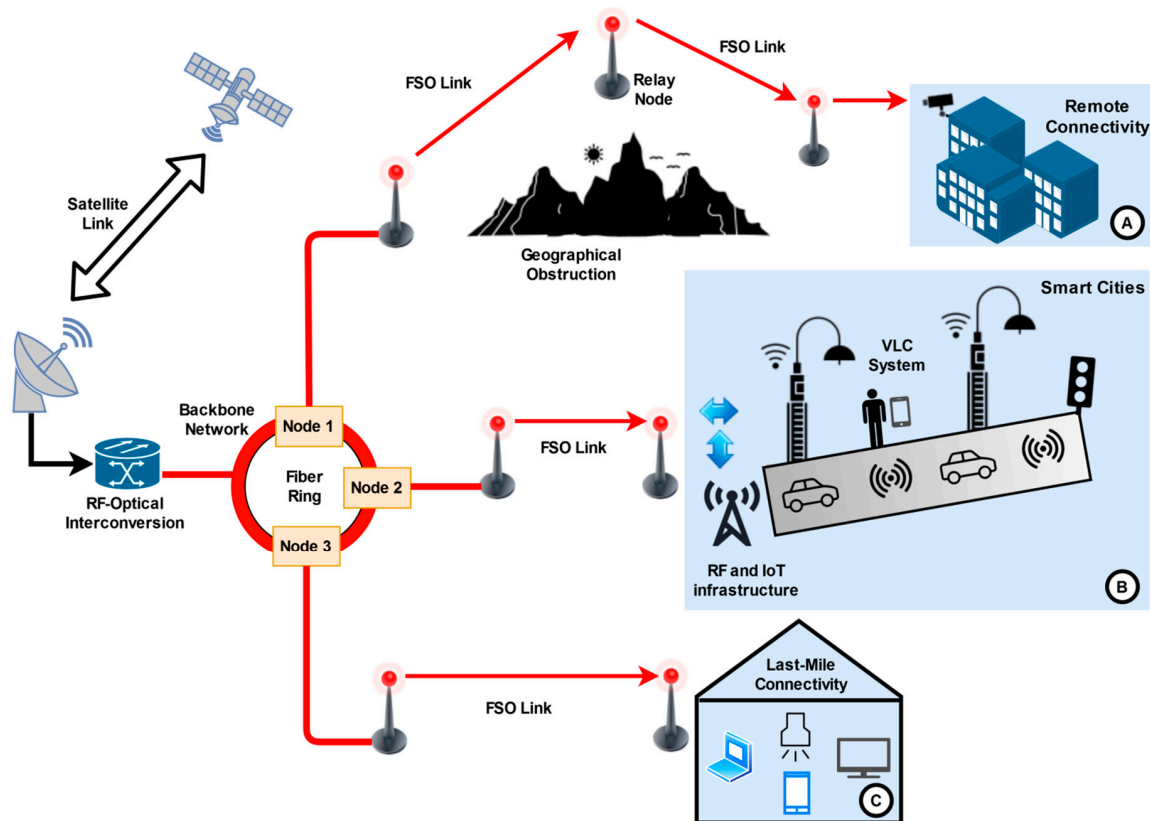


**Figure 2.** Smart city plan with optical connectivity to end-users.

Although 5G networks are being extensively being worked out to serve the needs of futuristic smart city systems, however, increasing bandwidth crunch will mean shifting towards millimeter-wave configuration. In such architectures, the RF links become increasingly directional, power-hungry and a reduction in serviceable range/area. As a result, the actual data rates may drop significantly as compared to theoretical ones [12]. The proposed link is, however, aimed at serving heterogeneous devices and networks through its ability to converge with backbone networks. The FSO link will, therefore, not only provide cost-effective connectivity on account of the use of unlicensed spectrum but also deliver data rates that, in a true sense much higher than the ones that can be achieved from 5G networks.

Despite the array of features and potential applications, FSO systems are yet to see large-scale commercial deployment. This is primarily because FSO is a LOS communication link where the atmosphere serves as the propagation medium, and thus, the presence of meteorological phenomena like rain, fog, snow, haze, and dust can result in significant signal degradation on account of absorption and scattering [1–4]. While the absorption of information-bearing photons leads to loss of power delivered at the receiver, scattering may lead to loss of LOS configuration, thus triggering erroneous data recovery at the receiver in both cases.

Furthermore, even on clear sunny days with negligible aerosols, FSO links can still suffer from a severe impairment. This impairment can be attributed to random fluctuations in the refractive index of the propagating medium and is commonly known as atmospheric turbulence. Temperature

fluctuations and/or mixing of hot and relatively cold air masses causes the formation of pockets of varying density known as eddies along the propagation path. The turbulence eddies, as shown in Figure 3, are capable of causing intensity and phase fluctuations in information-carrying photons, thus, at times leading to irreparable loss of information [7]. Over the years, various mathematical models like gamma–gamma, log-normal, k-distributed and negative exponential models have been investigated and proposed to characterize the impact of turbulence atmosphere on FSO signal [1,2]. Depending upon the severity of intensity scintillations caused to the presence of turbulence eddies, the turbulence may be categorized as weak, moderate or strong. While the log-normal model of best suited for received signal characterization during weak turbulence conditions, the negative exponential model is best suited for strong turbulence conditions only; however, the gamma–gamma model has been experimentally found to be approximately ideal for turbulence conditions ranging from weak to strong [1,3]. For the same reason, the performance analysis of the FSO link proposed here has been investigated, assuming that the channel is characterized by the gamma–gamma model.
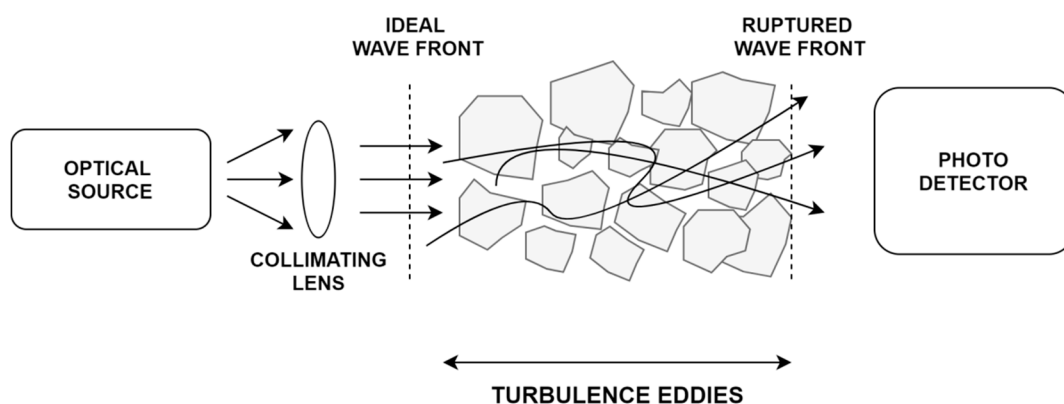
**Figure 3.** Formation of turbulence eddies leading to random fluctuation and ruptured wavefront in FSO links.

## 1.2. Literature Survey and Research Motivation

The process of modulating the information signal is an important aspect accomplished to achieve connectivity between the transceivers. The choice of modulation technique has a very critical role in determining the quality of the received signal and, subsequently, the information extraction at the receiver. Out of the various modulation techniques available, on–off keying (OOK) is most popular in FSO systems because of its sheer simplicity and cost-effective setup [3–5,13]. OOK-enabled FSO systems, however, perform miserably bad as channel conditions (turbulence) severity increases from weak to strong. Since atmospheric turbulence can cause unpredictable fluctuations in the intensity of the received signal; hence, amplitude modulated systems experience high bit error rates (BER) in such conditions [1–3]. The BER performance improvement in FSO links has been shown with the use of hybrid modulation schemes like pulse-position modulation (PPM) and sub-carrier modulation (SIM); however, the requirement of strict receiver coherence through carrier synchronization significantly add to system complexity and cost escalations [14–16]. Adaptive sub-carrier and polarization modulation schemes have also been reported to deliver seamless FSO link connectivity, but this virtue is limited only to moderately noisy and weak turbulence channels only [17,18]. Use of line coding techniques like a return to zero (RZ), non-return to zero (NRZ) and alternate mark inversion (AMI) along with modulation schemes like amplitude shift keying (ASK), OOK, PPM, etc. has also been proposed as a complementary measure to overcome the disastrous effect of channel turbulence [19,20]. Some higher-level modulation techniques like quadrature amplitude modulation (m-ary QAM) schemes with coherent detection have been reported for significant improvement in BER over turbulence FSO link; however, the main issue with coherent links is a requirement of carrier synchronization at the receiver, which adds to system complexity [21]. Apart from the choice of modulation schemes, diversity techniques have also

been found to be an effective tool in mitigating the effect of atmospheric turbulence in FSO links. As in radio-frequency (RF) based transmission, diversity refers to the transmission of modulated information over multiple channels to improve the link reliability. The temporal diversity, for example, involves the transmission of the same information multiple times with the objective of creating redundancy and the option to choose the best information packet at the receiver. This technique not only requires longer signal processing times but also leads to inefficient use of communication resources owing to redundant transmission required each time. Spatial diversity, on the other hand, overcomes this issue by using multiple transmitters and receivers, which will engage in simultaneous transmission of information, thus overcoming the delays experienced in time diversity systems. On the receiver side, there are three different techniques to combine the diversity signals, i.e., equal gain combining (EGC), maximal ratio combining (MRC) and selection combining (SC). Both EGC and MRC require precise phase information in order to ensure the constructive addition of received signals, thus making this system a complicated one. SC meanwhile uses the receiver branch with the highest signal-to-noise ratio (SNR) among all the branches, which is equivalent to selecting the branch with the highest light intensity making it much easy, simple and less complex. T. Joseph et al. in their paper [22], proposed the use of OOK FSO links with spatial diversity and reported performance enhancement over weak and moderate turbulence regimes; however, it was also reported that for overcoming turbulence regimes, the number of receivers should be increased which in turn may increase system complexity. Pham Tien Dat et al. in their paper [23], proposed optical wireless communication system integrated with the mm-wave system for 5G network. They used the OFDM technique for high-speed indoor communication. They have transmitted 40 Gbps radio signals over the 100 GHz band. However, the OFDM technique needs a transmitter and receiver to be coherent, which makes its architecture complex. Similarly, Nguyen et al., in their research work [24], investigated and put forward an idea of microwave photonic link, which integrates optical fiber, FSO and radio link to deliver all-time link connectivity. The idea in [24] is about using a modulation format that can ensure seamless connectivity among different communication networks.

Thus, for the same reasons as discussed here, we investigated the performance of the FSO link using different modulation formats, benchmarked with OOK, which are simple, cost-effective and user-friendly. The modulation formats were chosen with the intent to develop an FSO framework that can readily converge with different communication networks. Furthermore, spatial diversity with two transmitters and two receiver configurations ($2 \times 2$) was also used to strengthen the system performance over the turbulence channel. The rest of the paper is categorized into the following different sections. Section 2 elaborates on the turbulence theory. Section 3 provides the mathematical analysis of different modulation techniques, while the investigation results are reported in Section 4. Finally, the concluding remarks can be found in Section 5.

## 2. System Design

*Atmospheric Turbulence and Gamma–Gamma Channel*

Random variations in pressure and temperature along the propagation path cause the refractive index ($\eta$) of the medium to vary abruptly, thus leading to scintillation losses. *Turbulence theory*: The optical field radiation traversing in the atmosphere experiences the intensity and wavefront, as shown in Figure 3. Mathematically, the refractive index at any distance $L$ in space is related to channel parameters in the following manner [25]

$$\eta\left(L\right) = 1 + 77.6 \frac{\text{P}(L)}{\text{T}_{\text{e}}(L)} \times 10^{-6} \tag{1}$$

where P is the atmospheric pressure in millibars, $\text{T}_{\text{e}}$ is the temperature in Kelvin. The variations in channel refractive index of the medium, also known as optical turbulence, can be mathematically related to temperature in-homogeneities by the parameter $C_n^2$, also known as the refractive index

structure parameter. Although the value of $C_n^2$ varies with altitude (h) and wind velocity (v) as well as shown in Equation (2) [25],

$$C_n^2(\text{h}) = 0.00594\left(\frac{\text{v}}{27}\right)^2 \left(10^{-5}\right)^{10} \exp\left(\frac{-\text{h}}{1000}\right) + 2.7 \times 10^{-16} \exp\left(\frac{-\text{h}}{1500}\right) + A\left(\frac{-\text{h}}{100}\right) \qquad (2)$$

where Â is the nominal value of $C_n^2$ (0) at the ground in m$^{-2/3}$, and h is the altitude in meters. For the sake of analytical simplicity, $C_n^2$ can be written as a function of temperature structure constant $C_T^2$ as:

$$C_n^2 = \left(79 \times 10^{-6}\text{P}/\text{T}^2\right)^2 C_T^2 \qquad (3)$$

As a general rule of channel characterization in FSO links, $C_n^2$ defines the severity of turbulence strength. $C_n^2$ in the typical range of $10^{-12}$ m$^{-2/3}$ signifies strong turbulence conditions while $C_n^2$ in the range of $10^{-15}$ m$^{-2/3}$ and $10^{-17}$ m$^{-2/3}$ signify moderate and weak turbulence regimes [1,7].

Various channel models have been proposed in the recent past to mathematically quantify the impact of channel turbulence on the received signal. Out of the different proposed turbulence models, the gamma–gamma channel model is considered to be most reliable because this model exhibits close to ideal convergence between analytical and experimental results for all forms of turbulence regimes, i.e., strong, moderate and weak. This model considers the effect of small scale (scattering) and large scale (refraction) eddies of the propagating optical signal. The probability density function (PDF) of received light intensity (*I*) as determined from the gamma–gamma function can be represented as [1,8,9].

$$P(I) = \frac{2(\alpha\beta)^{\frac{\alpha+\beta}{2}}}{\Gamma(\alpha)\Gamma(\beta)} I^{\left(\frac{\alpha+\beta-2}{2}\right)} k_{\alpha-\beta}\left(2\sqrt{\alpha\beta I}\right); \; I > 0 \qquad (4)$$

where, $\alpha$ and $\beta$ represent the effective number of large- and small-scale eddies, respectively. $k_n$ (.) is the modified Bessel function of the 2nd kind of order ($\alpha - \beta$), and $\Gamma$ (.) represents the gamma function. The parameters $\alpha$ and $\beta$ can be individually written as a function of Rytov variance $\sigma_R$ as:

$$\alpha = \left[\exp\left(\frac{0.49\sigma_R^2}{\left(1 + 1.11\sigma_R^{\frac{12}{5}}\right)^{\frac{7}{6}}}\right) - 1\right]^{-1} \qquad (5)$$

$$\beta = \left[\exp\left(\frac{0.51\sigma_R^2}{\left(1 + 0.69\sigma_R^{\frac{12}{5}}\right)^{\frac{5}{6}}}\right) - 1\right]^{-1} \qquad (6)$$

where, $\sigma_R^2 = 1.23 C_n^2 k^{7/6} L^{11/6}$, here, $L$ is propagation channel length and $k$ is propagation constant, $2\pi/\lambda$. BER of an optical signal in the gamma–gamma channel can be determined using:

$$P_e = \int_0^\infty P\left(I^2\bar{\gamma}\right)P(I)dI \qquad (7)$$

where, $P\left(I^2\bar{\gamma}\right)$ represents the signal-to-noise ratio (SNR) at the receiver, while $P(I)$ is probability density function (PDF) of received irradiance of FSO link through the gamma–gamma channel model as expressed in Equation (4).

## 3. Modulation Techniques

In this section, we shall discuss various modulation techniques that will be used to analyze the performance of the proposed FSO link under different turbulence regimes.

### 3.1. On–Off Keying

OOK can use either non-return-to-zero (NRZ) or return-to-zero (RZ) pulse formats. In NRZ-OOK, the absence of peak optical represents a digital symbol "0", whereas the transmission of an optical pulse of peak power $P_T$ represents a digital symbol "1".

BER of OOK is given by:

$$P_{OOK} = Q\left(\sqrt{\frac{E_b}{2N_0}}\right) \tag{8}$$

where $E_b/N_0$ is referred to as SNR per bit.

The average energy per bit $E_b$ calculated as $E_b = 2(RP_r)^2 T_b$, where R is photodetector responsivity, $P_r$ is average received optical signal power, $T_b$ is bit duration, and $N_0/2$ is double-sided power spectral density determined as, $N_0 = 2qI_B$, where, $q$ is the electron charge, and $I_B$ is the average photocurrent generated by the background light.

The performance of the OOK-modulated FSO link under different turbulence regimes can be determined by substituting P(I) from Equation (4) and bit error rate from Equation (8) into Equation (7). Using different values of the refractive index structure $C_n^2$, Rytov variance ($\sigma^2$) for different channel conditions can be determined. The $\sigma^2$ can be further used to calculate the impact of turbulence eddies represented by $\alpha$ and $\beta$ in Equations (4) and (6), respectively. The received irradiance (P(I)) can then be calculated and substituted further in Equation (7).

Using the procedure explained here, the link performance of the FSO link for the rest of the optical modulation formats explained in Equations (9)–(13) can also be determined by using them in Equation (7).

### 3.2. Binary Phase-Shift Keying

BPSK is the simplest form of PSK where the carrier phase represents only two-phase states. BER of BPSK is given by:

$$P_{BPSK} = \frac{1}{2}\text{erfc}\left(\sqrt{\frac{E_b}{N_0}}\right) \tag{9}$$

### 3.3. Differential Phase-Shift Keying

DPSK modulation technique combines the PSK technique with differential encoding. In DPSK, the phase of the signal is advanced by 180° when symbol 1 is transmitted while it remains unchanged during symbol 0 transmissions. BER of DPSK is given by:

$$P_{DPSK} = \frac{1}{2}\exp\left(-\frac{E_b}{N_0}\right) \tag{10}$$

### 3.4. Gaussian Minimum Shift Keying

GMSK is the modulation technique where the frequency of the carrier wave (Gaussian pulse shape) is varied in accordance with the modulating signal. BER of GMSK is given by:

$$P_{GMSK} = Q\left(\sqrt{\frac{2\delta E_b}{N_0}}\right), \ \delta = 0.68 \tag{11}$$

### 3.5. Quadrature Amplitude Modulation

In QAM, the amplitude and phase of the carrier wave are varied in accordance with the message signal with a capacity of transmitting k bits of information.

$$k = \log_2 M; \text{ where, } k = 16, 64, 256 \text{ bits}$$

For 16-QAM, M $= 16$, k $= \log_2 16 = 4$bits

BER of GMSK is given by:

$$P_{QAM} = \frac{3}{2k} \text{erfc}\left( \sqrt{\frac{kE_b}{10N_0}} \right) \tag{12}$$

### 3.6. Dual Header-Pulse Interval Modulation (DH-PIM)

DH-PIM is the modified form of pulse interval modulation, which empty slots between two pulses. In DH-PIM, pulses of different lengths are used in the head slot. Slot error of DH-PIM is given by:

$$P_{se,DHPIM} = \frac{\left(\frac{3\alpha}{2}\right)\left[1 + \text{erf}\left\{\frac{(b-\sqrt{S_t})}{\sqrt{2\sigma_n^2}}\right\}\right] + \left[\frac{(4L-3\alpha)}{2}\right]\left[1 - \text{erf}\left(b - \sqrt{\sigma_n^2}\right)\right]}{4L} \tag{13}$$

## 4. Results and Discussions

Using Equations (4) and (7)–(13), we shall investigate the BER performance of the proposed FSO link using different modulation techniques discussed previously. The performance of the link was analyzed for turbulence conditions ranging from weak to strong. The investigation reported in this section can be broadly divided into two cases, links without spatial diversity and links with spatial diversity. Although it is well established from the reported literature that OOK modulated links are simple to design but lack the necessary fidelity, especially when the turbulence conditions vary from moderate to strong, however for the sake of quantitative comparison, we have considered the OOK scheme apart from other modulation techniques as well. Various link parameters that were used during the design and analysis of the proposed link are listed in Table 1.

**Table 1.** Link design parameters.

| Parameter | Range/Value |
|:---:|:---:|
| Link length [26,27] | 1.25 km |
| Refractive index structure ($C_n^2$) [28–30] | $10^{-12}$ m$^{-2/3}$ (strong turbulence) |
| | $10^{-15}$ m$^{-2/3}$ (moderate turbulence) |
| | $10^{-17}$ m$^{-2/3}$ (weak turbulence) |
| Spatial diversity order [26,31] | $2 \times 2$ |
| Photodetector responsivity [27,32] | 1 A/W |
| Operating wavelength [27,30,32,33] | 1550 nm |
| data rate ($r_b$) [3] | 155 Mbps |
| Transmitter aperture [27,34] | 20 cm |
| Receiver aperture [34,35] | 20 cm |

For single-channel FSO link operating in weak turbulence conditions, the BER performance of different modulation techniques for varying receiver SNR (dB) is shown in Figure 4. Similar investigation has also been extended to moderate and strong turbulence conditions as shown in Figures 5 and 6, respectively. For all the cases of FSO link without space diversity reception technique (SDRT) shown in Figures 4–6, we observe that out of all the investigated modulation formats, BPSK exhibits outstanding BER performance, followed very closely by 256-QAM and GMSK. Table 2 provides greater insight into the performance of different modulation formats in FSO links for weak, moderate and strong turbulence link conditions. Table 2 and Figure 4 shows that to achieve target BER of $10^{-8}$, OOK requires 19.9 dB SNR at the receiver, while the observed SNR requirements for DPSK, GMSK, 256-QAM, and BPSK are 10 dB, 9.2 dB, 8.4 dB, and 8 dB, respectively. The performance improvement of BPSK over OOK in a

weak turbulence scenario is approximately 59%. Figure 5 shows the BER performance of different modulation techniques in the moderate turbulence channel. To achieve the BER of $10^{-8}$, the SNR requirements for OOK, DPSK, BPSK, GMSK, and 256 QAM are 33 dB, 15.3 dB, 14.3 dB SNR, 16.8 dB SNR, and 15.1 dB, respectively. The performance improvement of BPSK over OOK in the moderate turbulence scenario is approximately 56%. A similar characteristic of BER performance is also seen in Figure 6, where, in the strong turbulence scenario to achieve the BER of $10^{-8}$, the SNR requirements for BPSK were the least at 19.5 dB while DPSK, GMSK, and 256-QAM had their SNR requirements at 21.5 dB SNR, 23 dB SNR, and 21 dB SNR, respectively. Hence, BPSK performs better than all other modulation techniques in all turbulence regimes channels, providing a significant SNR gain of almost 25 dB over OOK, even under strong turbulence conditions. Hence, the performance improvement of BPSK over OOK in a weak turbulence scenario is approximately 54%.
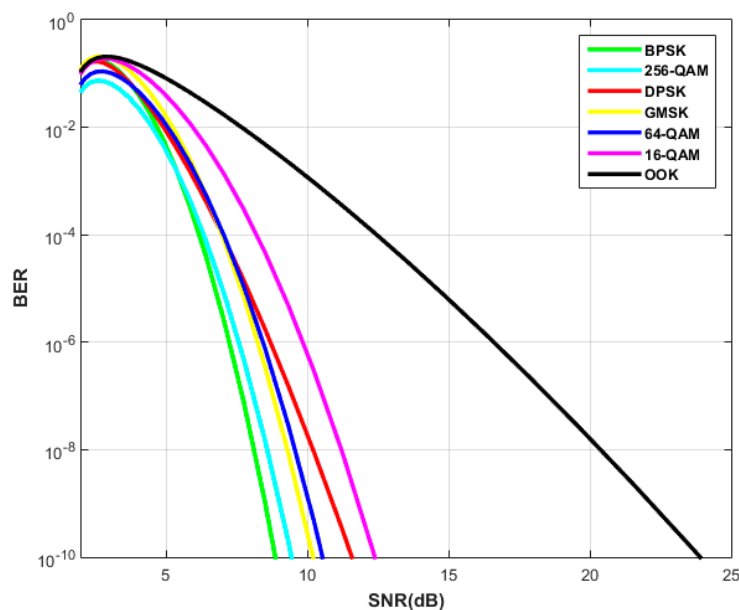


**Figure 4.** Bit error rate (BER) performance of different modulation formats without space diversity reception technique (SDRT) in a weak turbulence channel.
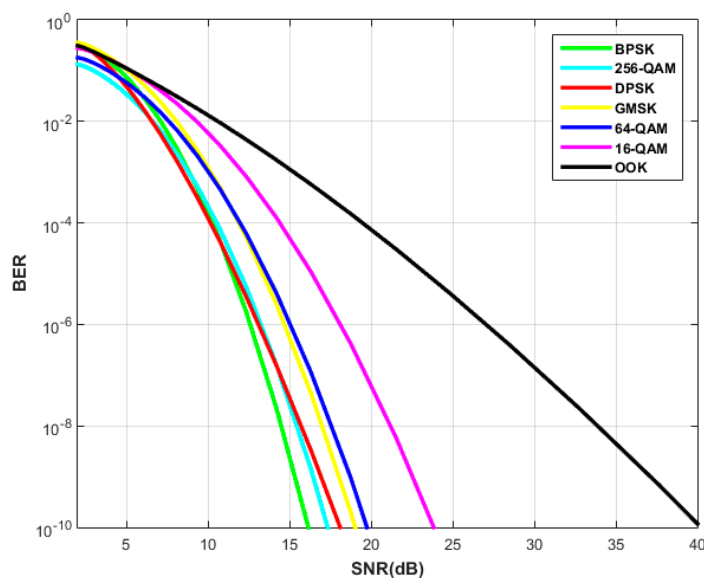


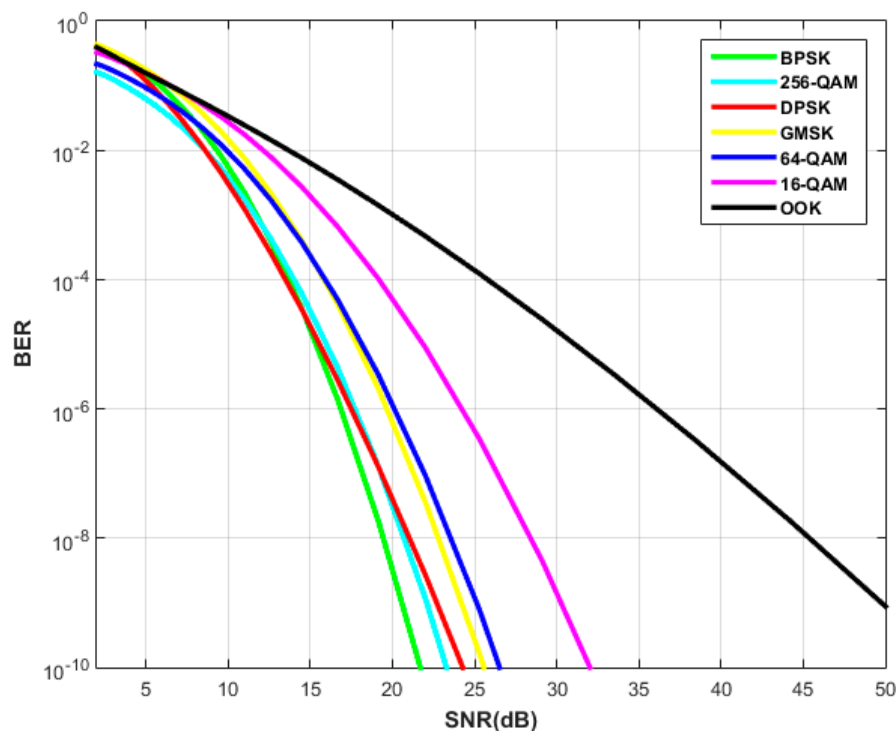**Figure 5.** BER performance of different modulation formats without SDRT in a moderate turbulence channel.

**Figure 6.** BER performance of different modulation formats without SDRT in a strong turbulence channel.

**Table 2.** SNR values (in dB) for modulation techniques without SDRT at BER $10^{-8}$ for weak, moderate and strong regimes.

| Modulation Technique | Weak Turbulence | Moderate Turbulence | Strong Turbulence |
|---|---|---|---|
| OOK | 19.9 | 33 | 45.2 |
| DPSK | 10 | 15.3 | 21.5 |
| BPSK | 8 | 14.3 | 19.5 |
| 256 QAM | 8.4 | 15.1 | 21 |
| 64 QAM | 9.4 | 17.3 | 23.5 |
| 16 QAM | 11 | 20.7 | 28 |
| GMSK | 9.2 | 16.8 | 23 |

Figure 7 shows the BER performance of different modulation techniques with $2 \times 2$ SDRT order and streamline the BER comparison single-channel link, i.e., without SDRT, which has also been illustrated in this figure. Significant SNR gain is observed in Figure 7 when SDRT links are compared with/without SDRT ones. To achieve the BER of $10^{-8}$ spatial diversity, OOK needs 8.8 dB SNR, and this SNR falls significantly to 5.1 dB in the case of the $2 \times 2$ BPSK link. Therefore, from the analysis, it can be seen that the FSO links with spatial diversity deliver improved SNR gains in contrast to single-channel links. The BER analysis discussed in Figure 7 was extended to moderate and strong turbulence conditions in Figures 8 and 9, respectively. Table 3 outlines the performance of different modulation techniques under various turbulence regimes for FSO links with and without spatial diversity. It may be seen from Table 3 that under all possible cases discussed here, it is the BPSK modulation technique that requires minimum SNR (dB) at the receiver to deliver the target BER performance. Furthermore, decent SNR gains (dB) are observed across all modulation formats when single-channel links are complimented with SDRT.
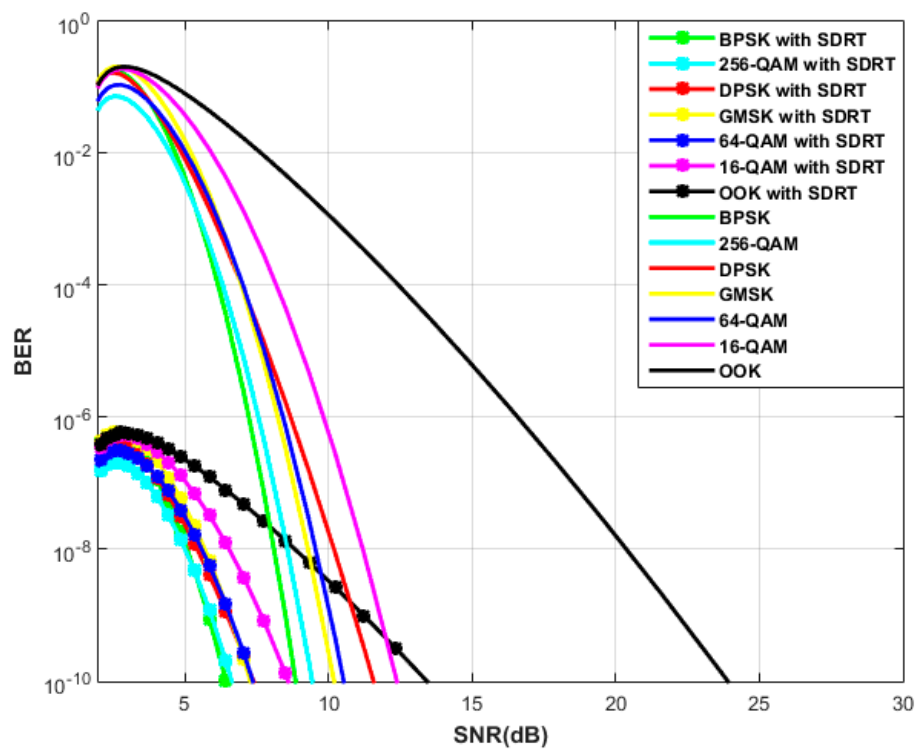
**Figure 7.** BER performance of different modulation formats with SDRT and without SDRT in a weak turbulence channel.
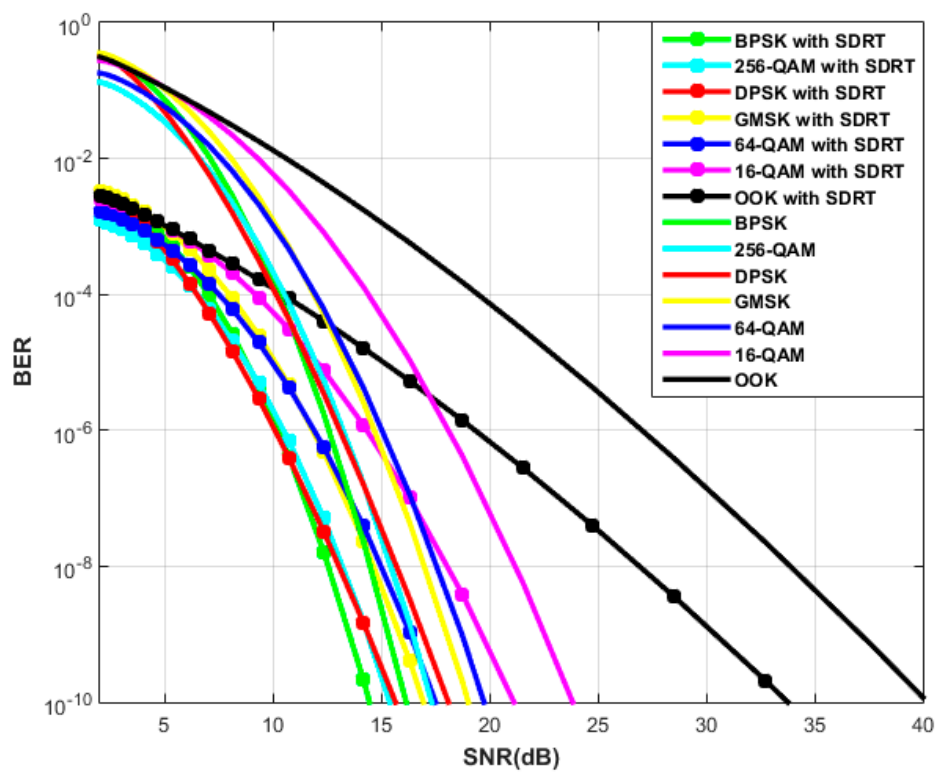


**Figure 8.** BER performance of different modulation formats with SDRT and without SDRT in a moderate turbulence channel.
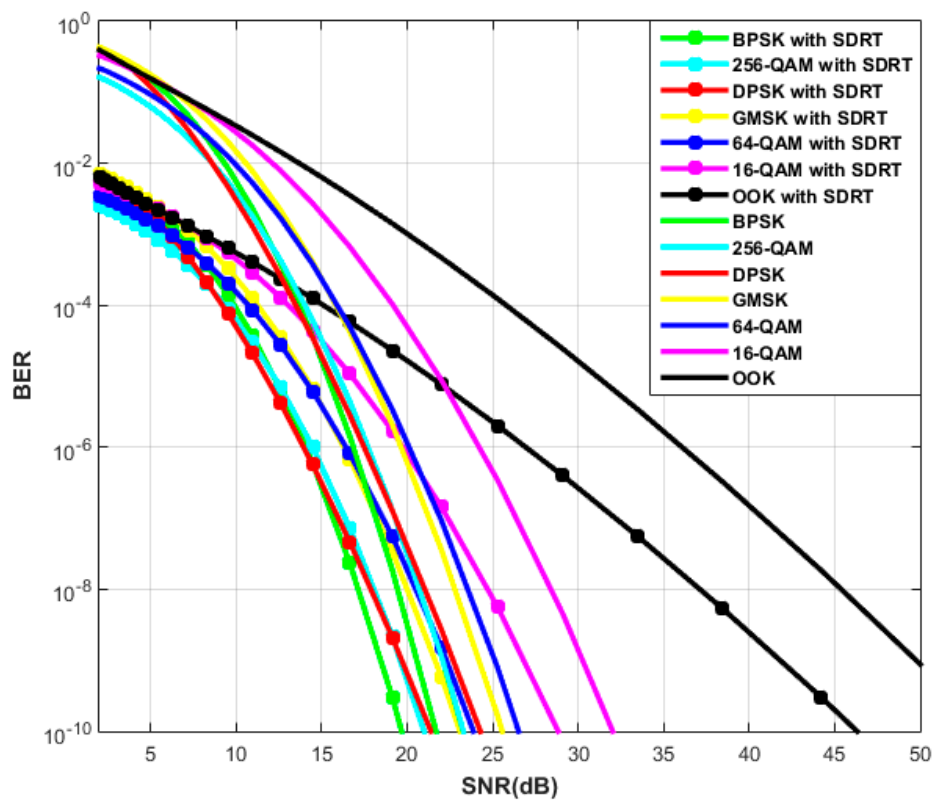
**Figure 9.** BER performance of different modulation formats with SDRT and without SDRT in a strong turbulence channel.

**Table 3.** SNR values (in dB) for modulation techniques with SDRT and without SDRT at BER $10^{-8}$ for Weak, moderate and strong regimes.

| Modulation Technique | Weak Turbulence Regime | | | Moderate Turbulence Regime | | | Strong Turbulence Regime | | |
|---|---|---|---|---|---|---|---|---|---|
| | Without SDRT (dB) | With SDRT (dB) | SNR Gain (%) | Without SDRT (dB) | With SDRT (dB) | SNR Gain (%) | Without SDRT (dB) | With SDRT (dB) | SNR Gain (%) |
| OOK | 19.9 | 8.8 | 55.7 | 33 | 26 | 21.2 | 45.2 | 37.2 | 17.69 |
| DPSK | 10 | 5.25 | 47.5 | 15.3 | 13 | 15 | 21.5 | 18 | 16.27 |
| BPSK | 8 | 5.1 | 36.25 | 14.3 | 12.5 | 12.5 | 19.5 | 17 | 12.82 |
| 256 QAM | 8.4 | 5 | 40.47 | 15.1 | 13.2 | 12.5 | 21 | 18.2 | 13.33 |
| 64 QAM | 9.4 | 5.6 | 40.42 | 17.3 | 15 | 13.2 | 23.5 | 20.2 | 14.04 |
| 16 QAM | 11 | 6.5 | 40.9 | 20.7 | 18 | 13 | 28 | 24.8 | 11.42 |
| GMSK | 9.2 | 5.7 | 38 | 16.8 | 14.6 | 13 | 23 | 20 | 13.04 |

$$\text{Percentage (\%)gain} = \frac{(\text{Gain without SDRT in regime}) - (\text{Gain with SDRT in regime})}{\text{Gain without SDRT in regime}} \times 100 \quad (14)$$

Figures 10–12 highlights the BER performance of DH-PIM with and without SDRT under weak, moderate, and strong turbulence channels. To achieve the target BER of $10^{-8}$, DH-PIM modulated FSO link without SDRT will require 79 dB SNR at the receiver which falls to 32 dB in presence of spatial diversity thus yielding a significant gain of approximately 47 dB. Similarly, as seen from Table 4, under moderate and strong turbulence conditions, the SNR gain achieved with SDRT is 17 dB and 11 dB, respectively.
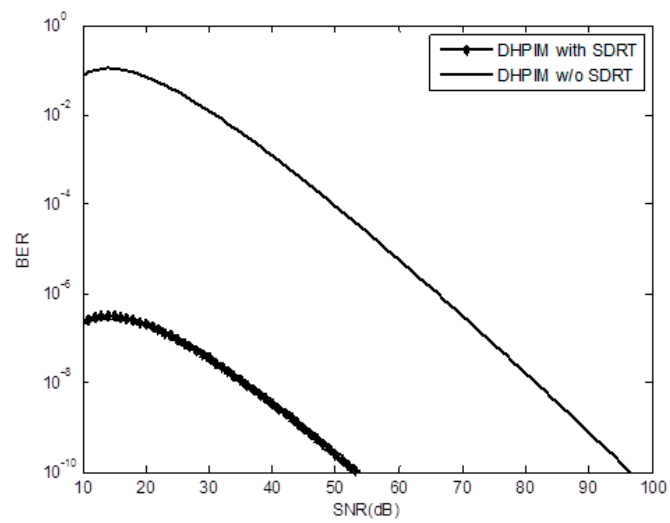
**Figure 10.** BER performance of dual header-pulse interval modulation (DH-PIM) with SDRT and without SDRT in a weak turbulence channel.
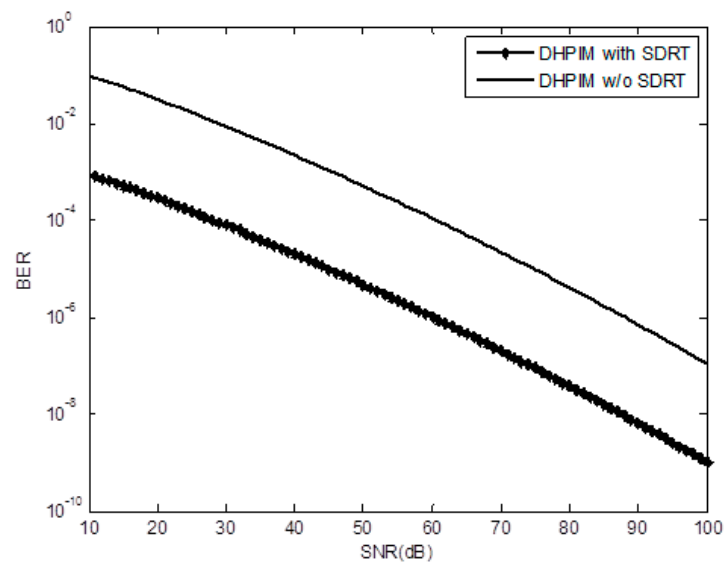


**Figure 11.** BER performance of DH-PIM with SDRT and without SDRT in a moderate turbulence channel.
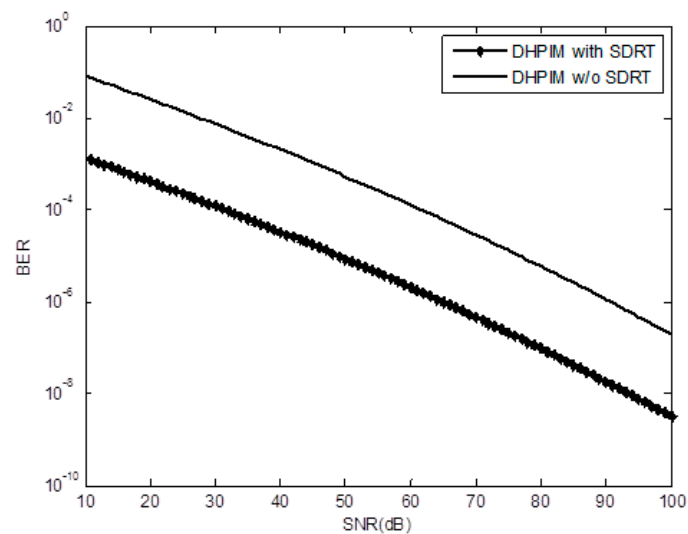


**Figure 12.** BER performance of DH-PIM with SDRT and without SDRT in a strong turbulence channel.

**Table 4.** SNR values (in dB) for DH-PIM with SDRT and without SDRT at BER $10^{-8}$ for weak, moderate and strong regimes.

| Modulation Technique | Weak Regime | Moderate Regime | Strong Regime |
|---|---|---|---|
| DH-PIM without SDRT | 79 | Above 100 | Above 100 |
| DH-PIM with SDRT | 32 | 83 | 89 |

## 5. Conclusions

During the analysis of the BER performances of different modulation techniques at various turbulence scenarios, i.e., weak, moderate and strong, it can be concluded that BPSK modulated links delivered an improved SNR gain of more than 10 dB over OOK links operated under similar conditions. Additionally, with the spatial diversity technique, BPSK modulated links witnessed further improvement in SNR gain to up to 25 dB over moderate and strong regimes. Furthermore, it can be concluded that among different modulation techniques investigated here, the BPSK FSO link combined with the $2 \times 2$ space diversity technique gives improved BER performance of 42% over others. The techniques used in the above analysis are simplex modulation techniques, which are very cost-effective. With the help of these techniques, we can integrate a set of devices into smart cities. With the considered link design parameters such as 155 Mbps of transmission speed, over 1 km of link range and moderate diversity order, the proposed link will be capable enough to support a hybrid communication model with last-mile capabilities. Moreover, for areas with rough and hostile terrain, where setting up RF infrastructure or digging fibers is very difficult, the proposed 1.2 km-long FSO links can be used in serial arrangement to reach out to the end-users. In the future, these modulation techniques can also be integrated with FEC techniques for further improvement in the links.

**Author Contributions:** Conceptualization, S.C., R.M.; Data curation, S.C., R.M.; Formal analysis, S.C., R.M.; Investigation, S.C. and R.M.; Methodology, S.C., R.M., L.K., G.S.G., and M.M.; Resources, M.M.; Visualization, L.K. and G.S.G.; Writing—original draft, S.C. and R.M.; Writing—review & editing, L.K., G.S.G., and M.M. All authors have read and agreed to the published version of the manuscript.

**Conflicts of Interest:** The authors declare no conflict of interest.

## References

1. Khalighi, M.A.; Uysal, M. Survey on free space optical communication: A communication theory perspective. *IEEE Commun. Surv. Tutor.* **2014**, *16*, 2231–2258. [CrossRef]
2. Miglani, R.; Malhotra, J.S. An innovative approach for performance enhancement of 320 Gbps free space optical communication system over turbulent channel. *Opt. Quant. Electron.* **2019**, *51*, 289. [CrossRef]
3. Ghassemlooy, Z.; Popoola, W.; Rajbhandari, S. *Optical Wireless Communications: System and Channel Modelling with Matlab®*; CRC Press: Boca Raton, FL, USA, 2019.
4. Institution of Engineering and Technology. *Principles and Applications of Free Space Optical Communications*; Majumdar, A.K., Ghassemlooy, Z., Raj, A.A.B., Eds.; IET: Stevenage, UK, 2019; pp. 1–330. Available online: https://digital-library.theiet.org/content/books/te/pbte078e (accessed on 30 October 2020).
5. Ramasarma, V. Free space optics: A viable last-mile solution. *Bechtel Telecommun. Tech. J.* **2002**, *1*, 22–30.
6. Majumdar, A.K. *Optical Wireless Communications for Broadband Global Internet Connectivity: Fundamentals and Potential Applications*; Elsevier: Amsterdam, The Netherlands, 2019; pp. 39–53.
7. Miglani, R.; Malhotra, J.S.; Majumdar, A.K.; Tubbal, F.; Raad, R. Multi-hop relay based free space optical communication link for delivering medical services in remote areas. *IEEE Photonics J.* **2020**, *12*, 1–21. [CrossRef]
8. Liu, Q.; Qiao, C.; Mitchell, G.; Stanton, S. Optical wireless communication networks for first-and last-mile broadband access. *J. Opt. Netw.* **2005**, *4*, 807–828. [CrossRef]

9.  Chowdhury, M.Z.; Shahjalal, M.; Hasan, M.; Jang, Y.M. The Role of optical wireless communication technologies in 5G/6G and IoT solutions: Prospects, directions, and challenges. *Appl. Sci.* **2019**, *9*, 4367. [CrossRef]

10. Nguyen, T.; Nguyen-Huu, D.; Nguyen, T. On achievable rate region using location assisted coding (LAC) for FSO communication. In Proceedings of the IEEE 86th Vehicular Technology Conference (VTC-Fall), Toronto, ON, Canada, 24–27 September 2017; pp. 1–5.

11. Pathak, P.H.; Feng, X.; Hu, P.; Mohapatra, P. Visible light communication, networking, and sensing: A survey, potential and challenges. *IEEE Commun. Surv. Tutor.* **2015**, *17*, 2047–2077. [CrossRef]

12. Minoli, D.; Occhiogrosso, B. Practical Aspects for the Integration of 5G Networks and IoT Applications in Smart Cities Environments. *Wirel. Commun. Mob. Comput.* **2019**, *6*, 1–30. [CrossRef]

13. Wang, Z.; Zhong, W.D.; Fu, S.; Lin, C. Performance comparison of different modulation formats over free-space optical (FSO) turbulence links with space diversity reception technique. *IEEE Photonics J.* **2009**, *1*, 277–285. [CrossRef]

14. Das, S.; Chakraborty, M. ASK and PPM modulation based FSO system under varying weather conditions. In Proceedings of the 2016 IEEE 7th Annual Ubiquitous Computing, Electronics & Mobile Communication Conference (UEMCON), New York City, NY, USA, 20–22 October 2016; pp. 1–7. Available online: https://ieeexplore.ieee.org/document/7777825 (accessed on 30 October 2020).

15. Dubey, D.; Prajapati, Y.K.; Tripathi, R. Error performance analysis of PPM-and FSK-based hybrid modulation scheme for FSO satellite downlink. *Opt. Quant. Electron.* **2020**, *52*, 286. [CrossRef]

16. Sharma, K.; Grewal, S.K. Performance assessment of hybrid PPM–BPSK–SIM based FSO communication system using time and wavelength diversity under variant atmospheric turbulence. *Opt. Quant. Electron.* **2020**, *52*, 1–25. [CrossRef]

17. Singh, M.; Malhotra, J. Performance investigation of high-speed FSO transmission system under the influence of different atmospheric conditions incorporating 3-D orthogonal modulation scheme. *Opt. Quant. Electron.* **2019**, *51*, 285. [CrossRef]

18. Saber, M.J.; Keshavarz, A. On performance of adaptive subcarrier intensity modulation over generalized F–SO links. In Proceedings of the Iranian Conference on Electrical Engineering (ICEE), Mashhad, Iran, 8–10 May 2018; pp. 358–361.

19. Badar, N.; Jha, R.K. Performance comparison of various modulation schemes over free space optical (FSO) link employing Gamma–Gamma fading model. *Opt. Quant. Electron.* **2017**, *49*, 192. [CrossRef]

20. Singh, M.; Malhotra, J. Performance comparison of different modulation schemes in high-speed MDM based radio over FSO transmission link under the effect of atmospheric turbulence using aperture averaging. *Wirel. Pers. Commun.* **2020**, *111*, 825–842. [CrossRef]

21. Singya, P.K.; Kumar, N.; Bhatia, V.; Alouini, M.S. On the Performance Analysis of Higher Order QAM Schemes over Mixed RF/FSO Systems. *IEEE Trans. Veh. Technol.* **2020**, *69*, 7366–7378. [CrossRef]

22. Joseph, T.; Kaushal, H.; Jain, V.K.; Kar, S. Performance analysis of OOK modulation scheme with spatial diversity in atmospheric turbulence. In Proceedings of the 2014 23rd Wireless and Optical Communication Conference (WOCC), Newark, NJ, USA, 9–10 May 2014; pp. 1–3.

23. Dat, P.T.; Kanno, A.; Inagaki, K.; Umezawa, T.; Yamamoto, N.; Kawanishi, T. Hybrid optical wireless-mmWave: Ultra high-speed indoor communications for beyond 5G. In Proceedings of the IEEE INFOCOM 2019—IEEE Conference on Computer Communications Workshops (INFOCOM WKSHPS), Paris, France, 29 April–2 May 2019; pp. 1003–1004.

24. Nguyen, D.-N.; Bohata, J.; Spacil, J.; Dousek, D.; Komanec, M.; Zvanovec, S.; Ghassemlooy, Z.; Ortega, B. M-QAM transmission over hybrid microwave photonic links at the K-band. *Opt. Express* **2019**, *27*, 33745–33756. [CrossRef]

25. Andrews, L.C. *Field Guide to Atmospheric Optics*, 2nd ed.; SPIE Press: Bellingham, WA, USA, 2001; p. 99.

26. Al-Gailani, S.A.; Mohammad, A.B.; Shaddad, R.Q.; Sheikh, U.U.; Elmagzoub, M.A. Hybrid WDM/multibeam free-space optics for multigigabit access network. *Photon. Netw. Commun.* **2015**, *29*, 138–145. [CrossRef]

27. Nor, N.A.M.; Ghassemlooy, Z.; Zvanovec, S.; Khalighi, M.; Bhatnagar, M.R. Comparison of optical and electrical based amplify-and-forward relay-assisted FSO links over gamma-gamma channels. In Proceedings of the 10th International Symposium on Communication Systems, Networks and Digital Signal Processing (CSNDSP), Prague, Czech Republic, 20–22 July 2016; pp. 1–5.

28. Pham, T.V.; Pham, T.A. Performance analysis of amplify-decode-and-forward multihop binary phase-shift keying/free-space optical systems using avalanche photodiode receivers over atmospheric turbulence channels. *IET Commun.* **2014**, *8*, 1518–1526. [CrossRef]

29. Libich, J.; Komanec, M.; Zvanovec, S.; Pesek, P.; Popoola, W.O.; Ghassemlooy, Z. Experimental verification of an all-optical dual-hop 10 Gbit/s free-space optics link under turbulence regimes. *Opt. Lett.* **2015**, *40*, 391–394. [CrossRef]

30. Aghajanzadeh, S.M.; Uysal, M. Multi-hop coherent free-space optical communications over atmospheric turbulence channels. *IEEE Trans. Commun.* **2011**, *59*, 1657–1663. [CrossRef]

31. Prabu, K. Analysis of FSO systems with SISO and MIMO techniques. *Wirel. Pers. Commun.* **2019**, *105*, 1133–1141. [CrossRef]

32. Trinh, P.V.; Dang, N.T.; Pham, A.T. Optical amplify-and-forward multihop WDM/FSO for all-optical access networks. In Proceedings of the 2014 9th International Symposium on Communication Systems, Networks & Digital Sign (CSNDSP), Manchester, UK, 23–25 July 2014; pp. 1106–1111.

33. Gao, Z.; Liu, H.; Ma, X.; Lu, W. Performance of multi-hop parallel free-space optical communication over gamma–gamma fading channel with pointing errors. *Appl. Opt.* **2016**, *55*, 9178–9184. [CrossRef] [PubMed]

34. Dabiri, M.T.; Sadough, S.M.S. Performance analysis of all-optical amplify and forward relaying over log-normal FSO channels. *J. Opt. Commun. Netw.* **2018**, *10*, 79–89. [CrossRef]

35. Alnajjar, S.H.; Noori, A.A.; Moosa, A.A. Enhancement of FSO communications links under complex environment. *Photonic Sens.* **2017**, *7*, 113–122. [CrossRef]